Graphical Abstract

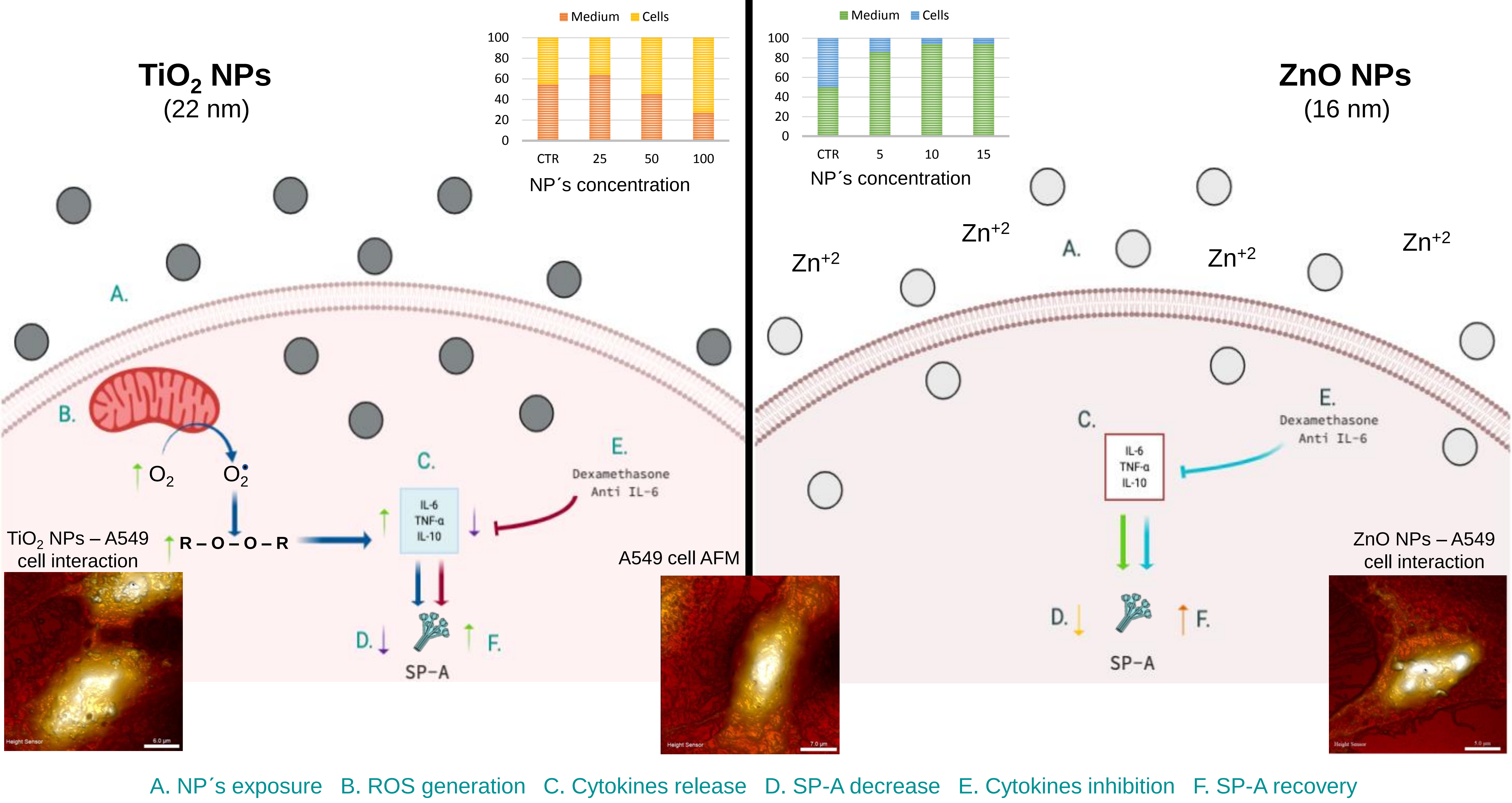

Highlights

TiO_2 NPs increase ROS generation and IL-6 release.

ZnO NPs increase the release of IL-6.

Increased IL-6 levels decrease the SP-A expression.

TiO_2 NPs biopersistence in cells may increase long term alveolar injury.

SP-A may be a good biomarker for the loss of lung function.

Inflammatory response in human alveolar epithelial cells after TiO_2 NPs or ZnO NPs exposure: inhibition of surfactant protein A expression as an indicator for loss of lung function

Authors:

A. Jiménez-Chávez[a], A. Solorio-Rodríguez[a,b], V. Escamilla-Rivera[c], D. Leseman[f], R. Morales-Rubio[a], M. Uribe-Ramírez[a], L. Campos-Villegas[d], I. E. Medina-Ramirez[e], L. Arreola-Mendoza[d], F.R. Cassee[f], A. De Vizcaya-Ruiz[a]*

[a]Departamento de Toxicología, Centro de Investigación y de Estudios Avanzados del IPN (CINVESTAV-IPN), Ciudad de México, México.

[b]Current address Environmental Health Science and Research Bureau, Health Canada, Ottawa, Canada.

[c]Departament of Otolaryngology – Head & Neck Surgery, College of Medicine, University of Arizona, Tucson, AZ 85724, USA

[d]Departamento de Biociencias e Ingenieria, Centro Interdisciplinario de Investigaciones y Estudios sobre Medio Ambiente y Desarrollo del IPN (CIIEMAD-IPN), Ciudad de México, México.

[e]Departamento de Química, Centro de Ciencias Básicas, Universidad Autónoma de Aguascalientes, Aguascalientes, México.

[f]National Institute for Public Health and the Environment (RIVM), P.O. Box, 2720 BA Bilthoven, The Netherlands.

*Corresponding author:

A. De Vizcaya-Ruiz

Avenida Instituto Politécnico Nacional No. 2508. Col. San Pedro Zacatenco, México D.F., C.P. 07360, México.

E-mail addresses: avizcaya@cinvestav.mx, avizcaya70@gmail.com

Keywords: Surfactant protein A, Interleukin 6, TiO_2 NPs, ZnO NPs, MONPs biopersistence.

Abstract

The increasing use of metal oxide nanoparticles (MONPs) as TiO_2 NPs or ZnO NPs has led to environmental release and human exposure. The respiratory system, effects on lamellar bodies and surfactant protein A (SP-A) of pneumocytes, can be importantly affected. Exposure of human alveolar epithelial cells (A549) induced differential responses; a higher persistence of TiO_2 in cell surface and uptake (measured by Atomic Force Microscopy) and sustained inflammatory response (by means of TNF-α, IL-10, and IL-6 release) and ROS generation were observed, whereas ZnO showed a modest response and low numbers in cell surface. A reduction in SP-A levels at 24 h of exposure to TiO_2 NPs (concentration-dependent) or ZnO NPs (the higher concentration) was also observed, reversed by blocking the inflammatory response (by the inhibition of IL-6). Loss of SP-A represents a relevant target of MONPs-induced inflammatory response that could contribute to cellular damage and loss of lung function.

1. Introduction

The growing use of engineered nanoparticles (NPs) in consumer products has caused an increase in their synthesis and manufacture. Up to September 2020 more than 4600 products containing nanomaterials (NMs) are registered in the Nanodatabase ("The Nanodatabase," 2020). Metal oxide nanoparticles (MONPs) are some of the most used and synthesized NMs, since they have been designed with specific characteristics to improve cosmetic and personal care products, food, medicinal products and other applications (Moezzi et al., 2012; Ziental et al., 2020). This wide use of the MONPs has led to an increase in occupational exposure due to their release during production and manufacturing, and the course of use and recycling (Ding et al., 2017). Once NPs are released to the environment, humans are mainly exposed by inhalation, with ingestion or skin deposition being of lesser importance (Shi et al., 2013). Adverse effects of TiO_2 NPs or ZnO NPs after inhaled exposure have been reported in various biological models by different groups. *In vitro* approaches have been used for predictive strategies of NPs toxicity (Kumar et al., 2017), leading to an understanding of the NP's toxicity and interactions with biological systems. Until now, mainly the general toxicity mechanism for TiO_2 NPs or ZnO NPs and their possible different effects inside the cells have been studied. Processes such as autophagy, lysosomal dysfunction, calcium homeostasis, cytotoxicity or genotoxicity have been included in the analyses (Hackenberg et al., 2011; Huang et al., 2010; Stern et al., 2012). Being the oxidative and inflammatory responses the underlying mechanisms causing these effects (Braakhuis et al., 2020; Hadrup et al., 2019). However, less is known about the impact on pulmonary surfactants, which are critical to maintaining tissue elasticity needed for good lung function performance (Parra & Pérez-Gil, 2015). Surfactant protein A (SP-A) is one of the main proteins that constitute the pulmonary surfactant; SP-A has an important role in the biophysical properties and the innate immune response of the alveoli (Lopez-Rodriguez & Pérez-Gil, 2014). We hypothesize that a proinflammatory response adversely affects SP-A and that this is related to the persistence and solubility of a MONPs. We have used a commonly used alveolar cell (A549) and poorly (TiO_2) and moderate soluble (ZnO) MONPs for our investigations.

2. Materials and methods

2.1 Chemicals and nanoparticles

HAM's cell culture media, TiO_2 P25 NPs (Product number 718467) and ZnO NPs (Product number 677450) were purchased from Sigma Aldrich (St. Louis MO, USA). Fetal Bovine Serum was purchased from Gibco™. The 2,7-dichloro-fluorescein diacetate (DCFH-DA), propidium iodide and Mitosox™ Red were obtained from Invitrogen (Thermo Fisher Scientific, USA). All other chemicals used were obtained from commercial sources and were of the highest grade available.

2.2 NPs suspension

A stock suspension of 2 mg/mL TiO_2 P25 NPs in dd-water was prepared and sonicated at 40% of amplitude (tip sonicator Q125, Qsonica, USA) for 2.5 minutes in an ice bath before dilutions at 25, 50, 100, 150 and 200 μg/mL suspensions in 0.5% FBS cell culture media. A stock suspension of 0.3 mg/mL ZnO NPs in dd-water was prepared and sonicated at 40% of amplitude (tip sonicator Q125, Qsonica, USA) for 2 minutes in an ice bath before being diluted to 2.5, 5.0, 10, 15 and 20 μg/mL suspensions in 0.5% FBS cell culture media. All suspensions were prepared under aseptic conditions.

2.3 NPs physicochemical characterization

One drop of either TiO_2 NPs or ZnO NPs aqueous was placed on a 300-mesh Cu grid for transmission electron microscopy (TEM) JEM-ARM 200F (JEOL Ltd, Japan) examination, for particle morphology and size distribution in TEM mode and elemental mapping by energy-dispersive X-ray spectroscopy (EDX). The particle size distribution of pristine NPs was calculated from the diameter of the individual particles distributed on diverse TEM micrographs. The hydrodynamic diameter was determined by dynamic light scattering analysis, DLS (Zetasizer NanoZS90 de Malvern Instruments Ltd, UK.), nanoparticle tracking analysis, NTA (NANOsight LM20, NANOSIGHT Ltd, UK), and CPS disc centrifugation, DC (DC24000UHR, CPS Instruments, USA); and Zeta potential by Laser Doppler microelectrophoresis in water and culture medium. Effective density of both NPs in different media was determined by volumetric centrifugation method (VCM) using the protocol described by DeLoid et al. (DeLoid et al., 2014).

2.4 NP endotoxin determination

The determination of endotoxin in TiO_2 NPs or ZnO NPs was performed with the Pierce™ Chromogenic Endotoxin Quant Kit (A39552) from Thermo Fisher Scientific, USA. The assay was done according to the manufacturer´s instructions. TiO_2 NPs or ZnO NPs dispersions were prepared at 1 mg/mL in endotoxin-free water.

2.5 Cell culture

The human type II alveolar epithelial cell line A549 was obtained from the American Type Culture Collection (CCL-185). A549 cells were cultured in Ham's F-12 cell culture media supplemented with 1% (v/v) penicillin, 1% (v/v) streptomycin, 1% (v/v) pyruvate, 1% (v/v) glutamine and 10% (v/v) inactivated FBS. Cells were maintained at 37ºC in a humidified atmosphere with 5% CO_2. Cells were seeded at 5 x 10^4 cells/cm^2 in 96- or 24-well plates and allowed to adhere 24 hours prior MONP exposure.

2.6 Metal ions concentration in cells and culture media

Atomic absorption spectrometry of Ti or Zn was performed to determine the metal ions concentration inside the A549 cells and in the culture media. The procedure was performed as described in Esquivel-Gaon et al. (2015). Briefly, after the exposure to the A549 cells to 3 different concentrations of TiO_2 NPs or ZnO NPs for 24 h, a sample of the culture media was obtained and centrifugated at 20 000 x g for 1 h and the supernatant was recovered as well as the NP pellet. The cells were washed with PBS and trypsinized, harvested and transferred to a clean tube. The cells and the exposure medium were subjected to two-stage digestion. After digestion Ti or Zn content was determined by atomic absorption spectroscopy (AAS).

2.7 NPs and A549 cells interaction determined by Atomic Force Microscopy

To determine the interaction between the A549 cells and the TiO_2 NPs or ZnO NPs cells were seeded on glass coverslips and exposed to increasing concentrations of NPs. After 24 h of exposure, coverslips with cells were washed twice with PBS and fixed with 10% formalin solution for 2 h. Then, Atomic Force Microscopy (AFM) (Bruker) was performed in tapping mode. The morphology of the cells and the NPs uptake was examined by AFM in tapping mode; images were analyzed with the NanoScope Analysis software.

2.8 Cell viability

Cell viability was measured by propidium iodide (PI) incorporation using flow cytometry. Briefly, after exposure to 25 - 200 μg/mL of TiO_2 NPs or 2.5 - 20 μg/mL of ZnO NPs and incubation for 12, 24 or 48 h, cells were washed twice with PBS solution. After the washing procedure, cells were trypsinized and resuspended in 200 μL of PBS containing PI (1.5 μM). PI fluorescence intensity was collected through 610/20 bandpass in an LSRFortessa (BD Biosciences) flow cytometer.

2.9 Intracellular ROS generation

After TiO_2 NPs or ZnO NPs exposure for 3, 12 and 24 h intracellular reactive oxygen species (ROS) generation as peroxides and mitochondrial superoxide were determined with the fluorescent probes DCFH-DA and MitoSOX™ Red, respectively. After exposure to the different concentrations of the NPs, cells were washed twice with PBS, trypsinized and resuspended in medium with DCFH-DA (10 μM) or MitoSOX™ Red (5 μM). DCFH-DA and MitoSOX™ Red fluorescence intensity were collected through 530/30 bandpass and 670/LP long pass filter respectively in an LSRFortessa (BD Biosciences, USA) flow cytometer.

2.10 Cytokine quantification

Cytokine (TNF-α, IL-6 and IL-10) released into cell culture media were measured using a Multiplex assay kit (Millipore Milliplex Cat. no. HCYTOMAG-60K Millipore Corp) according to the manufacturer's protocol. Briefly, after 24 and 48 h of TiO_2 NPs or ZnO NPs exposure at 25-100 μg/mL and 5.0-15 μg/mL respectively, supernatants were collected, centrifuged at 20,000 x *g* for 15 min and incubated overnight at 4 ºC with antibody-conjugated fluorescent beads. Afterwards, samples were incubated with antibodies coupled to biotin followed by streptavidin-phycoerythrin incubation. All samples were read in the MAGPIX instrument (Luminex Corporation), and data analysis was performed with the xPONENT Software (Luminex Corporation).

2.11 SP-A protein level determination

To obtain the total protein, cells were homogenized with Nonidet-P40 buffer, sonicated in a bath sonicator for 5 min, and centrifuged at 20,000 x *g* for 10 minutes at 4ºC. Sample supernatants were obtained and stored at -70ºC until use. The protein concentration of samples was determined using the Bradford protein assay. A 2x Laemmli buffer was added to 50 μg of protein, and the sample was loaded in 12% SDS-polyacrylamide gel and transferred to a PVDF membrane. The membranes were blocked by 1 h with 5% non-fat milk. After blocking, the membranes were incubated overnight with primary antibody to SP-A (1:1000 mouse monoclonal SP-A antibody sc-80621). The blots were then incubated with HRP-labeled secondary antibodies (Bio-Rad Laboratories, Hercules, CA, USA) for 1 h at a dilution of 1:10000. The immunoreactivity was detected using Luminata Western blotting detection reagent (Millipore). The bands were registered with a C-DiGit® Blot Scanner (LI-COR Biosciences). An Actin antibody (1:500 mouse monoclonal Actin antibody sc-8432) was used as an internal control.

2.12 IL-6 inhibition

To inhibit the effect of the IL-6, a specific anti-IL-6 antibody (R&D Systems) treated with 200 μL of anti-IL-6 or 10 nM Dexamethasone simultaneous with TiO_2 NPs or ZnO NPs per 24h in the culture media to inhibit the IL-6 activity. After exposure to NPs cells were washed twice with PBS and obtained to extract the protein from the cells and determine the expression of the SP-A as mentioned in the previous section.

2.13 Statistical analysis

Results are expressed as means values ± Standard Error of the Mean (SEM). Data were analyzed by one-way ANOVA test followed by the Bonferroni *post hoc* test. For the obtained western blot results data were analyzed by U-Mann Whitney test. Data were considered significant at *$p< 0.05$ or **$p<0.001$. Statistical software Prism 6.0 (GraphPad Software, Inc. US).

3. Results

3.1 NPs characterization

The knowledge of physicochemical characteristics of TiO_2 NPs and ZnO NPs suspended in cell culture media used for biological assays are necessary to understand biological model response and NPs interaction. In this study the determination of physical characteristics showed that TiO_2 NPs exhibited a larger average primary size than ZnO NPs (Table 1) with a size distribution of 12 - 50 nm and 2 – 32 nm, respectively (data not shown); a semi-spherical shape and the formation of agglomerates for both NPs here studied (Figure 1). Relative density determination showed 1.90 mg/mL in water and 1.34 mg/mL in Ham's media for TiO_2 NPs; whilst for ZnO NPs a 1.58 mg/mL value in water and 1.49 mg/mL in Ham's media was observed. In dispersion, TiO_2 NPs in water and culture media appeared as a monodispersed stable suspension; showing a hydrodynamic diameter of 17 nm, a PDI value of 0.3 and a zeta potential of 0.16 mV in water; and in Ham's media a hydrodynamic diameter of 335 nm, a PDI value of 0.2 and a zeta potential of -12.07 mV. For ZnO NPs, the agglomerate formation was observed in water and culture media. ZnO NPs showed a hydrodynamic diameter of 278 nm, a 0.25 PDI value and a zeta potential of 30.56 mV in water; and in Ham's media a hydrodynamic diameter of 368 nm, a 0.6 PDI value and a zeta potential of -12.2 mV. A decrease in the average of the agglomerates size in Ham's media after 24 and 48 h (Table 1) was observed for ZnO NPs. TiO_2 NPs preserved their average hydrodynamic diameter and PDI in all the tested times. Additionally, the determination of the presence of endotoxin in the TiO_2 NPs and ZnO NPs surface was determined by the Chromogenic Endotoxin Quant Kit, the obtained results showed an endotoxin concentration of less than 0.1 UE/mL for both NPs (Table 1).

3.2 Metal ions concentration in cells and culture media

To determine the stability of TiO_2 NPs or ZnO NPs in cell culture media and their concentration inside the cells, the concentration of the Ti or the Zn ions was determined in the culture media and in the cells after acidic digestion. After 24 h of exposure to TiO_2 NPs Ti levels increased in a concentration-dependent manner inside the cells (Table 2). In the media the TiO_2 concentration were almost the same in all the tested concentrations suggesting a low Ti solubility released from TiO_2 NPs (a visible particle pellet was observed after centrifugation of the media with the NPs). On the other hand, exposure to ZnO NPs showed a higher proportion of Zn in the culture media compared to cells (Table 2); these cell media concentrations of Zn ions were determined in a concentration-dependent manner (Table 2), suggesting a high solubility of the ZnO NPs in the media and a low permanence in the system as part of the NP entity (compared with the TiO_2 NPs); although an increased concentration of Zn ions was determined in the cells in a concentration-dependent manner after 24 h of exposure. This release of particle elements could modify the interaction and the possible effects of the particles in the cells; therefore, we considered necessary to evaluate cell-NP interaction.

3.3 NPs and A549 cells interaction determined by Atomic Force Microscopy

The interaction and possible permanence of the NPs in the cells and the culture medium can contribute to the understanding of the effects and the cellular damage induced to the A549 cells after MONPs exposure. Based on this, the morphology of the cells, the presence of MONPs and the possible nano-bio interaction between the MONPs and the A549 cells were registered and examined using Atomic Force Microscopy (AFM). The samples were analyzed in tapping mode in air, and images were recorded using height, amplitude and phase channels. Figures 2 and 3, show the presence of agglomerated particles spread on the cell surface, and a concentration-dependent increase on the NPs-cell interaction. Figures 2A-C show the topography and phase images of non-treated A549 cells. The cells exhibit their characteristic (oblong shaped) morphology. At higher magnifications, fine details in the 2D representation of the cell can be distinguished. Phase images denote the presence of only biological tissue. Figures 2D-F show a magnification of the cell membrane of non-treated cells. In particular, phase imaging indicates the presence of only one material domain (cell). Analysis of the cells after interaction with MONPs indicates close interaction of MONPs with the cell membrane and possible internalization (Figures 2G-L and 3G-L) in contrast to the images of control A549 cells. The presence of agglomerates in the exposed cells images can demonstrate the presence and interaction of the TiO_2 NPs (Figure 2 G-I, circles) with the apical surface of A549 cells; in the same manner changes between the contrast shades of the different images (Figure 2 J-L, arrows) could suggest particles internalization. An increase in the number of particle agglomerates could be observed in a concentration-dependent manner on the A549 cell surface (Supplementary Figure 1). ZnO NPs-cells interaction showed small particle agglomerates on the A549 cells surface (Figure 3 G-I, circles), as well as the possible particles internalization given by the changes in the contrast shades from the different images (Figure 3 J-L). The increase of the agglomerates in a concentration-dependent manner was observed between the ZnO NPs and the cellular surface (Supplementary Figure 2). Once the NPs-cell interaction was demonstrated we followed to determine some of the biological effects induced by these MONPs.

3.4 Cell viability

The cytotoxic effect of the TiO_2 NPs or ZnO NPs on the A549 lung epithelial cells was determined using PI viability assays (Figure 4). Exposure to TiO_2 NPs showed a significant increase in necrosis in a time- and concentration-dependent manner (Figure 4A). From 12 h of exposure to TiO_2 NPs, a significant increase in cellular necrosis from the exposure to the concentration of 150 and 200 μg/mL was observed compared to the control. This effect was also observed after 24 and 48 h of exposure to 100, 150 and 200 μg/mL of TiO_2 NPs (Figure 4A). Despite the aforementioned, increase in the number of necrotic cells values are not considered as cytotoxic because levels of necrotic cells did not exceed 20% of death cells. On the other hand, the exposure to ZnO NPs did not show significant changes at any of the concentrations and times analyzed compared with the control cells with the PI assay analysis, showing that all the analyzed concentrations are non-cytotoxic for the A549 cells (Figure 4D).

3.5 Intracellular ROS generation

One of the starting points in the effects caused by some NPs is the stimulation of ROS intracellular generation. After TiO_2 NPs and ZnO NPs exposure on the A549 cells at non-cytotoxic concentrations, the intracellular superoxide and peroxides generation were determined (Figure 4). The mitochondrial superoxide anion production increased significantly after 3, 12 and 24 h of TiO_2 NPs exposure, this increase was observed in almost all the tested concentrations (Figure 4B). Similarly, a moderate increase of the peroxides formation was observed in all the analyzed time-points at different TiO_2 NPs concentrations (Figure 4C). Furthermore, the exposure to ZnO NPs in the times and concentrations analyzed did not show a difference in the generation of the superoxide anion and peroxides compared to the control cells (Figure 4E and F). As the following step, we decided to also assess the inflammatory response induction from the exposure to MONPs, with the main interest of investigating if TiO_2 NPs or ZnO NPs would have the ability to activate different pathways.

3.6 Inflammatory response determination by cytokine quantification

Lung damage or chronic injury as a consequence of a sustained or progressive inflammatory process can cause irreversible lesions. In Figure 5 the release of the different inflammatory cytokines, indicators of an inflammatory response, are presented after 24 and 48 h of exposure to TiO_2 NPs or ZnO NPs. During the exposure to TiO_2 NPs the increase of IL-6 release was observed with the highest concentration tested (100 μg/mL) and at both time points tested; TNF-α secretion showed an increase after 48 h exposure in all the NPs concentrations analyzed; and the release of the anti-inflammatory cytokine IL-10 that increased after 100 μg/mL exposure at 24 h (Figure 5A, B and C). On the other hand, exposure to ZnO NPs induced a significant secretion of IL-6 that increased after 24 h of NPs exposure at

15 μg/mL; the release of TNF-α increased after 48 h in the highest concentration assayed; and the concentration of IL-10 increased after 48 h of 10 μg/mL NPs exposure (Figure 5D, E and F). These findings confirm a concentration-dependent increase of the inflammatory response caused by MONPs exposure in A549 cells.

3.7 SP-A levels determination

The expression of the SP-A protein in type II alveolar epithelial cells is essential to maintaining tissue integrity and elasticity, and the primary immune defense (participating in the opsonization of external agents) in the alveolar region. Scarce information about the effect on the SP-A concentration after MONPs exposure is available; for this reason, after TiO_2 NPs or ZnO NPs exposure in non-cytotoxic concentrations, the level of SP-A was determined. Our results (Figure 6A) showed a significant reduction in the expression of SP-A after 24 h of exposure to TiO_2 NPs in the A549 cells in a concentration dependent manner. Meanwhile, after ZnO NPs exposure the expression of SP-A showed a significant decrease at 24 h in the 15 μg/mL concentration (Figure 6B). This decrease in the SP-A expression could affect the first line of defense of the alveoli increasing their susceptibility to external agents and causing the alveolar epithelium to collapse and thus consequent tissue damage.

3.8 IL-6 inhibition

Some studies suggest a possible relationship between the increase in the inflammatory response (specifically IL-6 increase) and the misregulation of surfactant proteins levels. To determine this relative dependence, we used a specific and a general inhibitor (anti-IL-6 and dexamethasone, respectively) to suppress IL-6 activity. In Figure 6A an increase of the SP-A level after the co-exposure of TiO_2 NPs (100 μg/mL) and anti-IL-6 or TiO_2 NPs (100 μg/mL) and dexamethasone, compared with the single exposure to TiO_2 NPs (100 μg/mL) can be noticed. In the same manner, in the co-exposure to ZnO NPs (15 μg/mL) and anti-IL-6 or ZnO NPs (15 μg/mL) and dexamethasone the levels of SP-A showed an increase compared to the exposure to ZnO NPs (15 μg/mL) (Figure 6B). It is important to mention that SP-A protein levels showed no difference compared with the control despite the presence of the TiO_2 NPs or the ZnO NPs when the inhibitors are present. This increase in the level of the SP-A after the co-exposure denotes the recovery of the protein by the inhibition of the IL-6, demonstrating the participation of IL-6 in the SP-A suppression process. The interaction of the effects caused by the MONPs and their specific damage can be appreciated; where in a general mode of action MONPs leads to an inflammatory response; and the specific increase of IL-6 levels may cause the disruption of specific cellular essential functions such as the SP-A expression.

4. Discussion

Understanding the hazard of NPs that can be released to the environment is a crucial aspect for assaying the health risk associated with exposure to these promising materials. Rapid low costs *in vitro* models provide valuable information about the cellular toxicity effects such as cell viability, ROS generation, and the inflammatory response. Here we demonstrated that SP-A should be added as a key marker to assess the impact on lung function.

Physical-chemical nanoparticle characterization in the biological media to be used in biological models is critical for the determination of their toxicity. The differential composition and properties of the NPs can induce a different uptake and mechanisms which will produce a different cellular response (Sukhanova et al., 2018). Despite the similarity of the TiO_2 NPs and the ZnO NPs characteristics at the beginning of the interaction in culture media; TiO_2 NPs characteristics remained with time, while ZnO NPs showed a change in the hydrodynamic diameter and solubility when the exposure time increased. The biopersistence of the TiO_2 NPs given their characteristics can contribute to long-term exposure of the A549 cells and sustained effects in the alveoli until NPs elimination, which could not happen since little particle clearance is known to occur in the alveoli. However, the solubility from the ZnO NPs and the increased Zn ion release in the media, as also other studies have reported (Ivask et al., 2015), opens the possibility of a reduced persistence in biological models, which can contribute to the ZnO NPs toxicity and a different type of induced cell injury compared with TiO_2 NPs.

The nano-bio interaction of both MONPs was determined by AFM; these images demonstrated the presence of the MONPs in contact with the A549 cells, and their relationship with the observed effects. This interaction and the differential persistence of the MONPs can contribute to the possible long-term effects; the nano-bio interaction of TiO_2 or ZnO NPs have been tested before by others. Images from Transmission Electron Microscopy (TEM) in a cellular model after 96 h of exposure showed the interaction of TiO_2 NPs but not ZnO NPs in ovarian cells, showing the ZnO NPs solubility in the culture media and possibly inside the cells (Santacruz-Márquez et al., 2020). The TiO_2 NPs biopersistence and interaction contributes to the toxicological effects, but also the long-term effects of the TiO_2 NPs compared to the ZnO NPs.

The NPs-cell interaction activates a series of responsive events inside the cell. Non-cytotoxic concentrations of MONPs are capable of producing or inducing ROS and activate a series of events which can lead to the damage of the cells or tissue integrity (Yu et al., 2020). The increase of intracellular ROS generation (superoxide anion and peroxides) from exposure to TiO_2 NPs in alveolar cells during all the tested temporalities showed a starting point of the mode of action of this NPs. This sustained effect caused by the persistence of NPs inside the cells and their ability to produce ROS has also been reported in other studies (Hanot-Roy et al., 2016; K. N. Yu et al., 2015). For ZnO NPs ROS generation was not observed in the tested temporalities. This finding has been previously reported by other authors, where the ZnO NPs can cause cellular toxicity without the ROS generation (He et al., 2017). The lack of the ROS generation can be associated with the ZnO NPs characteristics and poor stability in the culture medium and inside the cell ambience.

The initiation of the inflammatory response as a signal of cellular injury was observed after exposure to both MONPs. This inflammatory response was observed before from both MONPs in a short term determination (Simón-Vázquez et al., 2016). Despite both TiO_2 and ZnO NPs showed a concentration-dependent increase of TNF-α and IL-6 as part of the inflammatory response, only TiO_2 NPs showed a sustained increase of inflammatory markers. The differential effect in the inflammatory response could be due to the interaction but also to the concentration and permanence of the NPs in the biological media. The results suggest a specific inflammatory response due to the characteristics of the TiO_2 NPs, such as their persistence. Surprisingly for both MONPs exposures, a modest but statistically significant increase in the levels of anti-inflammatory IL-10 cytokine was observed. The release of IL-10 has been related with the anti-inflammatory response; plays an important role in limiting host immune response to pathogens, preventing damage to the host and maintaining tissue homeostasis (Kamaly et al., 2016). The presence of IL-10 after the MONPs exposure can be interpreted as a protective mechanism against the NPs damage to the cells. However, this presence of the IL-10 could be not enough to counteract the sustained damage produced by the TiO_2 NPs. It is necessary to study in a more specific manner the possible implications of the IL-10 in the MONPs exposure.

Furthermore, pulmonary surfactant production is one of the main functions of alveolar type II epithelial cells. The SP-A contributes to the biophysical function and innate immune response from the alveoli. A lack in the production of SP-A protein can lead to susceptibility of the alveoli to respiratory pathologies (respiratory distress syndrome, innate immune susceptibility, amongst others), external toxicants and microorganisms transmission (Lopez-Rodriguez et al., 2014). The exposure of the A549 cells to the MONPs induced a decrease in SP-A levels. The interaction of the NPs with the SP-A has been reported before (Arick et al., 2015). This possible SP-A-MONPs interaction given by the opsonin activity of SP-A can contribute to their decrease in the alveolar system. Also, the acute and subchronic exposure to particulate matter less than 2.5 microns (PM2.5), a relevant particulate pollutant, have shown a decrease of the SP-A in the lungs (Aztatzi-Aguilar et al., 2016). This decrement of SP-A and surfactant secretion could contribute to alveolar collapse, and also to an increase of cell susceptibility due to the lack of the innate defense response produced by this protein. The lack of SP-A after the continuous exposure to MONPs, could enhance tissue damage and the loss of the homeostasis; leading to cell death and finally promoting tissue fibrosis or tumor promotion scenarios (Braakhuis et al., 2020).

The inhibition of the inflammatory response by dexamethasone or specifically the inhibition of IL-6 by an antibody anti-IL-6 allowed to determine its contribution in the cellular damage observed (Mogensen et al., 2008; Dembek et al., 2016); and as other authors have reported, the addition of specific concentrations of the IL-6 in A549 cell culture media can induce the decrement in the SP-A levels during specific times (Doumanov et al., 2014). The co-exposure of the MONPs and the IL-6 inhibitors showed the restored of the level of the SP-A, demonstrating the participation of the IL-6 in this event, and showing how it is possible to ameliorate MONPs effect by the use of the specific inhibitors from the inflammatory response. However, it is necessary to determine the effectiveness and the duration of the inflammatory inhibitors in the biological systems, as well as, the possible effects from the other participants of the inflammatory response (TNF-α and IL-10) on the alveolar cells.

It is important to notice the interaction between the increased secretion of IL-6 by the A549 cells and the subsequent inhibition of the SP-A expression; as mentioned in the literature shown in our results, these two events are correlated and in our specific study the increased levels of IL-6 were induced by the presence of the MONPs. All the effects of the TiO_2 NPs or ZnO NPs can be associated with some of their physicochemical characteristics, which despite being similar at some point had an important difference, their persistence in the biological media. The proved solubility of the ZnO NPs (determined by other studies) could be the difference in the biological effects of these particles compared with TiO_2 NPs. The poor solubility or the persistence of the TiO_2 NPs in the biological system compared with the ZnO NPs can be related to their constant ROS generation and the sustained IL-6 secretion, but also to their effect in the SP-A expression decrease. Compared with the TiO_2 NPs effects, ZnO NPs showed some similar effects but of a short duration, which could allow the recovery of the cells. In the TiO_2 NPs case, the possible persistence of the NPs can trigger long-term effects in the biological system. This difference in the MONPs persistence in the biological model can be crucial in the understanding of the MONPs effects, where persistent particles can be associated to chronic inflammation, cellular damage and possibly to tissue injury leading to fibrosis and tumor promotion.

5. Conclusions

This study shows the relevance of the SP-A as a possible biomarker of the damage caused by NP's as well as of the loss of lung function. In the same manner, this work contributes to determining the physicochemical characteristics as the persistence and the solubility of the TiO_2 and ZnO NPs; which can contribute to the interaction with A549 cells and their adverse effects. Despite the similarity between some of the caused effects by both MONPs, the time course and the dose level at which these events occur are different. These differences in the temporalities and their sustained effect seem to be a consequence of the difference in cell uptake and dissolution of the MONPs. Finally, would be important to consider the use of SP-A as a marker to characterize the hazard of MONPs and can also be used as a valuable marker for grouping and read-across approaches for NPs categorization in nanosafety.

Author contributions

A.J.C. and A.D.V.R. designed the study; A.J.C., A.S.R, and D.L. performed the characterization of the nanoparticles; A.J.C., V.E.R., A.S.R., M.U.R. and R.M.R. performed *in vitro* experiments; A.J.C., L.A.M. and L.C.V. performed and analyzed the metal ions concentrations, A.J.C. and I.E.M.R. performed and analyzed the NPs and cells interaction by atomic force microscopy; A.J.C., A.D.V.R., and F.R.C.

performed the data analysis and wrote the manuscript. All the authors revised and approved the manuscript.

Acknowledgements

This work was partially funded by Conacyt [Consejo Nacional de Ciencia y Tecnología] Grant No. 167778, 286739 and PN-2017-01-4710. A.J.C. held a Conacyt graduate scholarship No. 780827.

6. References

Arick, D. Q., Choi, Y. H., Kim, H. C., & Won, Y. Y. (2015). Effects of nanoparticles on the mechanical functioning of the lung. *Advances in Colloid and Interface Science*, *225*, 218–228. https://doi.org/10.1016/j.cis.2015.10.002

Aztatzi-Aguilar, O. G., Uribe-Ramírez, M., Narváez-Morales, J., De Vizcaya-Ruiz, A., & Barbier, O. (2016). Early kidney damage induced by subchronic exposure to PM2.5in rats. *Particle and Fibre Toxicology*, *13*(1). https://doi.org/10.1186/s12989-016-0179-8

Braakhuis, H. M., Gosens, I., Heringa, M. B., Oomen, A. G., Vandebriel, R. J., Groenewold, M., & Cassee, F. R. (2020). Mechanism of Action of TiO 2 : Recommendations to Reduce Uncertainties Related to Carcinogenic Potential, 1–21.

Buerki-Thurnherr, T., Xiao, L., Diener, L., Arslan, O., Hirsch, C., Maeder-Althaus, X., … Krug, H. F. (2013). In vitro mechanistic study towards a better understanding of ZnO nanoparticle toxicity. *Nanotoxicology*, *7*(4), 402–416.

DeLoid, G., Cohen, J. M., Darrah, T., Derk, R., Rojanasakul, L., Pyrgiotakis, G., … Demokritou, P. (2014). Estimating the effective density of engineered nanomaterials for in vitro dosimetry. *Nature Communications*, *5*, 1–10.

Dembek, A., Laggai, S., Kessler, S. M., Czepukojc, B., Simon, Y., Kiemer, A. K., & Hoppstadter, J. (2016). Hepatic interleukin-6 production is maintained during endotoxin tolerance and facilitates lipid accumulation. *Immunobiology*, *222*(6), 786–796.

Ding, Y., Kuhlbusch, T. A. J., Van Tongeren, M., Jiménez, A. S., Tuinman, I., Chen, R., … Riediker, M. (2017). Airborne engineered nanomaterials in the workplace—a review of release and worker exposure during nanomaterial production and handling processes. *Journal of Hazardous Materials*, *322*, 17–28.

Doumanov, J., Jordanova, A., Zlatkov, K., Moskova-Doumanova, V., & Lalchev, Z. (2014). Investigation of IL-6 effects on SP-A expression in A549 lung cell line. *Biotechnology and Biotechnological Equipment*, *26*(June), 96–99.

Esquivel-Gaon, M., Anguissola, S., Garry, D., Gallegos-Melgar, A. del C., Saldaña, J. M., Dawson, K. A., … Del Razo, L. M. (2015). Bismuth-based nanoparticles as the environmentally friendly replacement for lead-based piezoelectrics. *RSC Adv.*, *5*(35), 27295–27304.

Hackenberg, S., Scherzed, A., Technau, A., Kessler, M., Froelich, K., Ginzkey, C., … Kleinsasser, N. (2011). Cytotoxic, genotoxic and pro-inflammatory effects of zinc oxide nanoparticles in human nasal mucosa cells in vitro. *Toxicology in Vitro*, *25*(3), 657–663.

Hadrup, N., Rahmani, F., Jacobsen, N. R., Saber, A. T., Jackson, P., Bengtson, S., … Vogel, U. (2019). Acute phase response and inflammation following pulmonary exposure to low doses of zinc oxide nanoparticles in mice. *Nanotoxicology*, *13*(9), 1275–1292. https://doi.org/10.1080/17435390.2019.1654004

Hanot-Roy, M., Tubeuf, E., Guilbert, A., Bado-Nilles, A., Vigneron, P., Trouiller, B., … Lacroix, G. (2016). Oxidative stress pathways involved in cytotoxicity and genotoxicity of titanium dioxide (TiO2) nanoparticles on cells constitutive of alveolo-capillary barrier in vitro. *Toxicology in Vitro*, *33*, 125–135.

He, T., Long, J., Li, J., Liu, L., & Cao, Y. (2017). Toxicity of ZnO nanoparticles (NPs) to A549 cells and A549 epithelium in vitro: Interactions with dipalmitoyl phosphatidylcholine (DPPC). *Environmental Toxicology and Pharmacology*, *56*(May), 233–240.

Huang, C. C., Aronstam, R. S., Chen, D. R., & Huang, Y. W. (2010). Oxidative stress, calcium homeostasis, and altered gene expression in human lung epithelial cells exposed to ZnO nanoparticles. *Toxicology in Vitro*, *24*(1), 45–55.

Ivask, A., Titma, T., Visnapuu, M., Vija, H., Kakinen, A., Sihtmae, M., … Kahru, A. (2015). Toxicity of 11 Metal Oxide Nanoparticles to Three Mammalian Cell Types In V.itro. *Current Topics in Medicinal Chemistry*, *15*(18), 1914–1929.

Kamaly, N., Fredman, G., Fojas, J. J. R., Subramanian, M., Choi, W. I., Zepeda, K., … Farokhzad, O. C. (2016). Targeted Interleukin-10 Nanotherapeutics Developed with a Microfluidic Chip Enhance Resolution of Inflammation in Advanced Atherosclerosis. *ACS Nano*, *10*(5), 5280–5292. https://doi.org/10.1021/acsnano.6b01114

Kumar, V., Sharma, N., & Maitra, S. S. (2017). In Vitro and In Vivo Toxicity Study of Nanoparticles. *International Nano Letter*.

Lai, X., Wei, Y., Zhao, H., Chen, S., Bu, X., Lu, F., … Zhang, J. (2015). The effect of Fe 2 O 3 and ZnO nanoparticles on cytotoxicity and glucose metabolism in lung epithelial cells. *Journal of Applied Toxicology*, *35*(6), 651–664.

Lopez-Rodriguez, E., & Pérez-Gil, J. (2014). Structure-function relationships in pulmonary surfactant membranes: From biophysics to therapy. *Biochimica et Biophysica Acta - Biomembranes*, *1838*(6), 1568–1585.

Moezzi, A., McDonagh, A. M., & Cortie, M. B. (2012). Zinc oxide particles: Synthesis, properties and applications. *Chemical Engineering Journal*, *185–186*, 1–22.

Mogensen, T. H., Berg, R. S., Paludan, S. R., & Østergaard, L. (2008). Mechanisms of dexamethasone-mediated inhibition of toll-like receptor signaling induced by Neisseria meningitidis and Streptococcus pneumoniae. *Infection and Immunity*, *76*(1), 189–197.

Parra, E., & Pérez-Gil, J. (2015). Composition, structure and mechanical properties define performance of pulmonary surfactant membranes and films. *Chemistry and Physics of Lipids*, *185*, 153–175.

Ramsés Santacruz-Márquez, Aidee Solorio-Rodríguez, Sirenia González-Posos, Jaime Santoyo-Salazar, Sihomara Patricia García-Zepeda, Andrea De Vizcaya-Ruiz, Isabel Hernández-Ochoa. Comparative effects of TiO2 and ZnO nanoparticles on growth and ultrastructure of ovarian antral follicles. Reproductive Toxicology (2020) Vol 96: 399-412.

Sahu, D., Kannan, G. M., Vijayaraghavan, R., Anand, T., & Khanum, F. (2013). Nanosized Zinc Oxide Induces Toxicity in Human Lung Cells, *2013*.

Shi, H., Magaye, R., Castranova, V., & Zhao, J. (2013). Titanium dioxide nanoparticles: a review of current toxicological data. *Particle and Fibre Toxicology*, *10*(1), 15.

Simón-Vázquez, R., Lozano-Fernández, T., Dávila-Grana, A., & González-Fernández, Á. (2016). Analysis of the activation routes induced by different metal oxide nanoparticles on human lung epithelial cells. *Future Science OA*, *2*(2). https://doi.org/10.4155/fso.16.2

Stern, S. T., Adiseshaiah, P. P., & Crist, R. M. (2012). Autophagy and lysosomal dysfunction as emerging mechanisms of nanomaterial toxicity. *Particle and Fibre Toxicology*, *9*(March), 20–35.

Sukhanova, A., Bozrova, S., Sokolov, P., Berestovoy, M., Karaulov, A., & Nabiev, I. (2018). Dependence of Nanoparticle Toxicity on Their Physical and Chemical Properties. *Nanoscale Research Letters*, *13*. https://doi.org/10.1186/s11671-018-2457-x

The Nanodatabase. (2020). Retrieved September 18, 2020, from https://nanodb.dk/en/

Yu, K. N., Chang, S. H., Park, S. J., Lim, J., Lee, J., Yoon, T. J., … Cho, M. H. (2015). Titanium dioxide nanoparticles induce endoplasmic reticulum stress-mediated autophagic cell death via mitochondria-associated endoplasmic reticulum membrane disruption in normal lung cells. *PLoS ONE*, *10*(6), 1–17.

Yu, Z., Li, Q., Wang, J., Yu, Y., Wang, Y., Zhou, Q., & Li, P. (2020). Reactive Oxygen Species-Related Nanoparticle Toxicity in the Biomedical Field. *Nanoscale Research Letters*, *15*(1). https://doi.org/10.1186/s11671-020-03344-7

Ziental, D., Czarczynska-Goslinska, B., Mlynarczyk, D. T., Glowacka-Sobotta, A., Stanisz, B., Goslinski, T., & Sobotta, L. (2020). Titanium dioxide nanoparticles: Prospects and applications in medicine. *Nanomaterials*, *10*(2).

Supplementary Table 1. Another NPs characterization.

NP	NTA size (nm)	CPS size (nm)
TiO_2	23 ± 118	66.9 ± 26.4
ZnO	38 ± 99	22.1 ± 7.6

Note: Values represent the mean ± standard deviation.

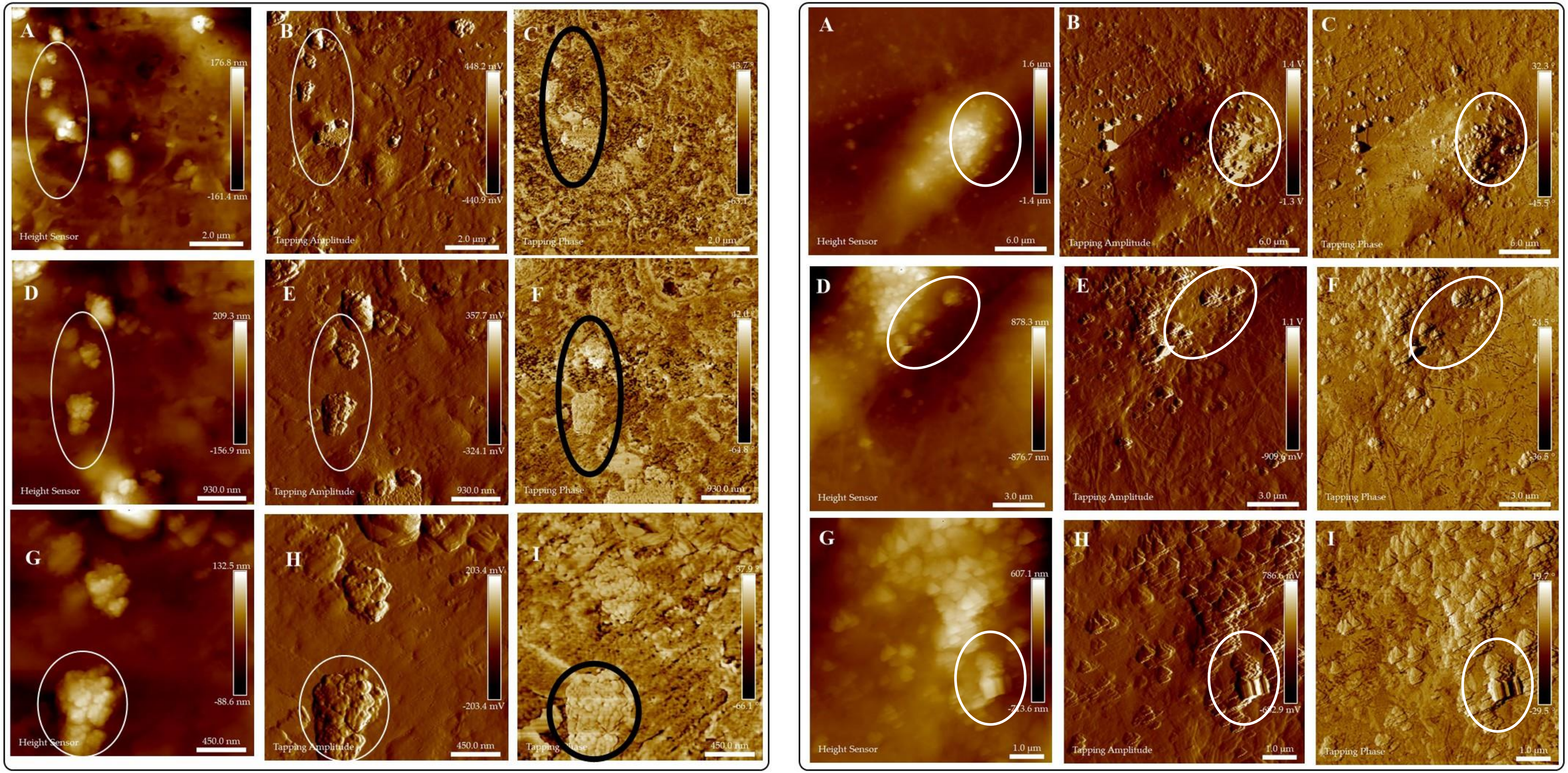

Supplementary Figure 1. Cell-NPs interaction. TiO_2 NPs interaction with A549 cells was dermined by AFM. The presence of TiO_2 NPs agglomerates (50 µg/mL and 100 µg/mL) inside the A549 cells can be seen in the images. Circles shows the NPs agglomerates and the changes in the contrast of the images.

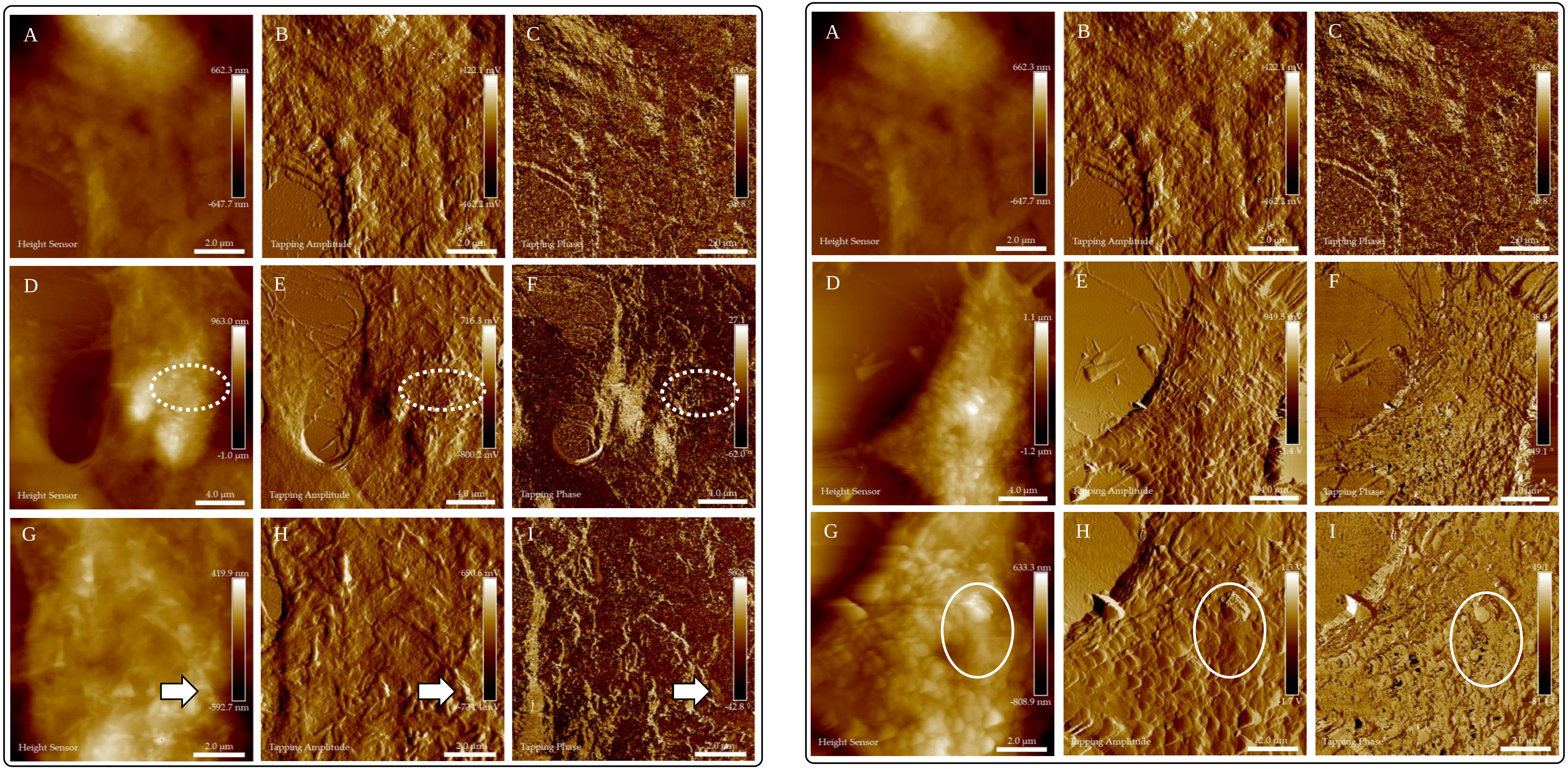

Supplementary Figure 2. ZnO NPs and A549 cells interaction. ZnO NPs interaction with A549 cells was dermined by AFM. The presence of ZnO NPs agglomerates (10 µg/mL and 15 µg/mL) can be seen covering the A549 cells. Circles shows the NPs agglomerates interacting with the cells

Figures Revised version

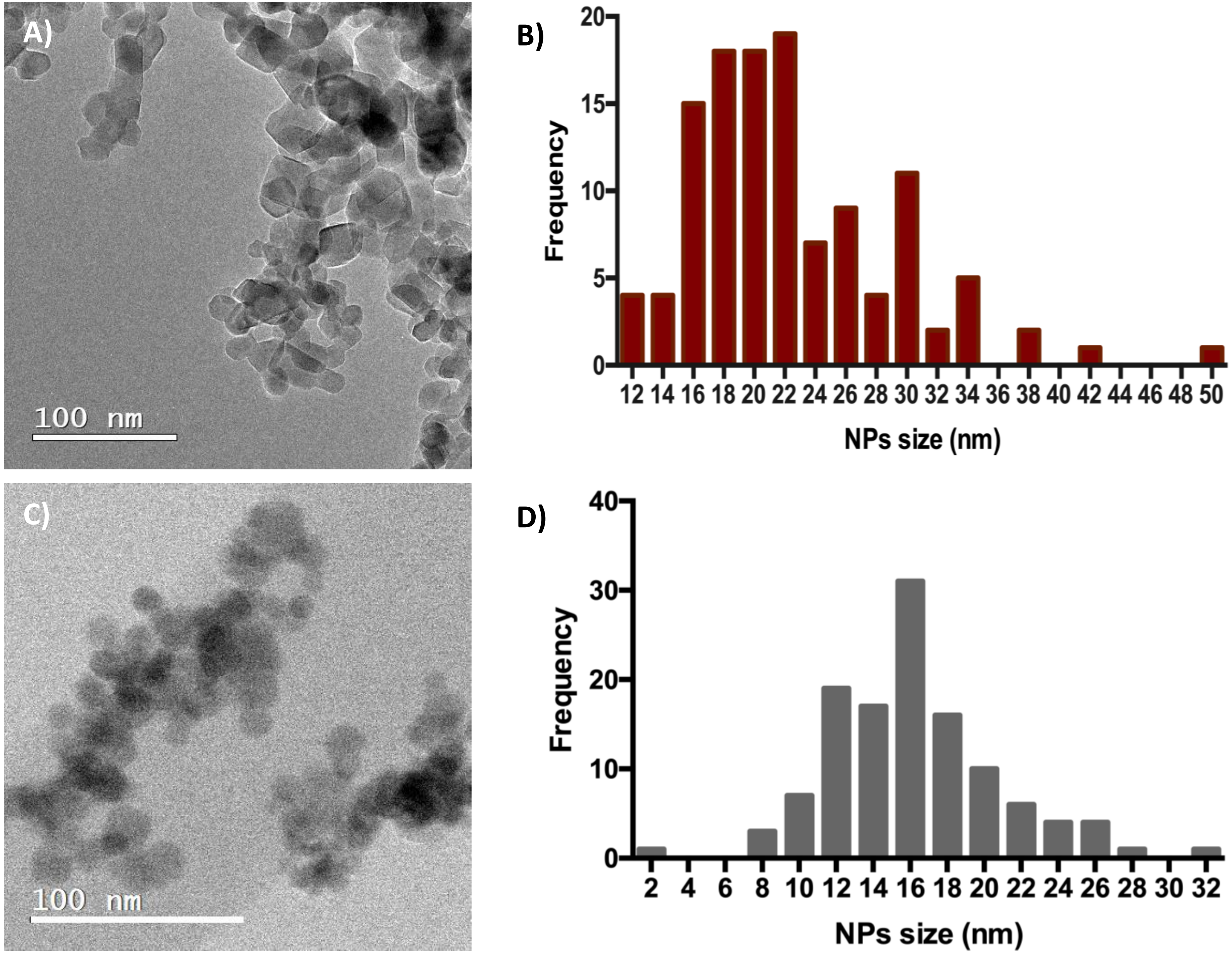

Figure 1. NPs characterization. TiO_2 NPs and ZnO NPs were characterized by transmission electron microscopy to determine the shape, agglomeration and primary size distribution. A) TiO_2 NPs TEM microraph, B) TiO_2 NPs primary size distribution graphic, C) ZnO NPs TEM microraph, ZnO NPs primary size distribution graphic.

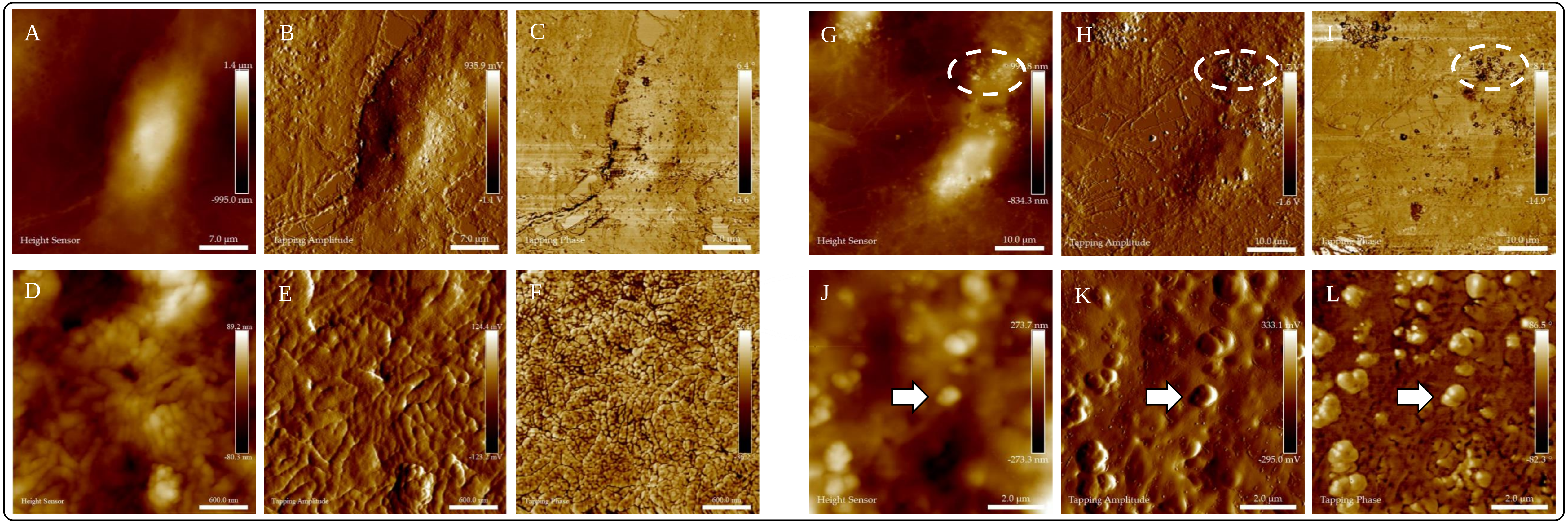

Figure 2. Interaction between TiO_2 NPs and A549 cells. Atomic Force Microscopy images from A549 cells or TiO_2 NPs – A549 cells interaction were obtained after 24 h of exposure. Representative images showed the morphology of the A549 cells (A – C) and their membrane surface (D – F). Disperse TiO_2 NPs (25 µg/mL) and their interaction with the cells can be seen by the contrast between the images inside the circle (G – I). Particles aglomerates inside the cell membrane (arrows) can be seen by the contrast between the images (J – L).

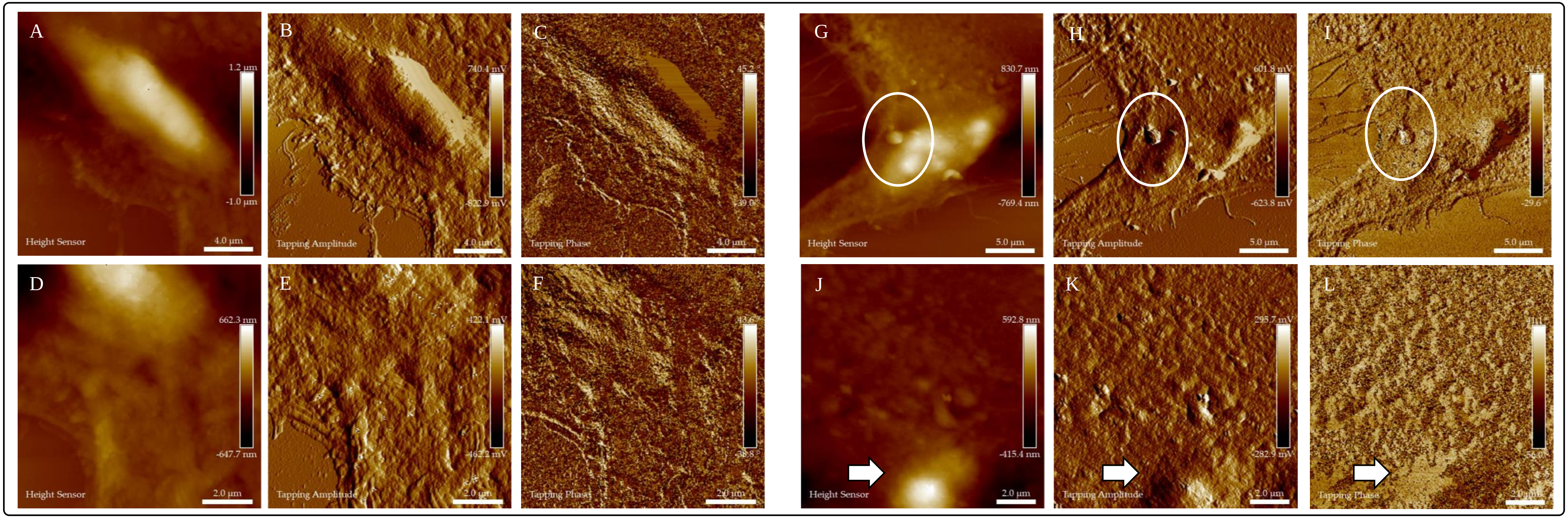

Figure 3. ZnO NPs and A549 cells interaction. The presence of the ZnO NPs (5 µg/mL) inside the A549 cells was determined by AFM after 24 h of exposure. Representative images showed the morphology (A – C) and the membrane surface of A549 cells (D – F). Circles shows the agglomerates of NPs interacting with the cell (D – F). Arrows shows a closer aproach of the agglomerates (G – I) inside the A549 cells.

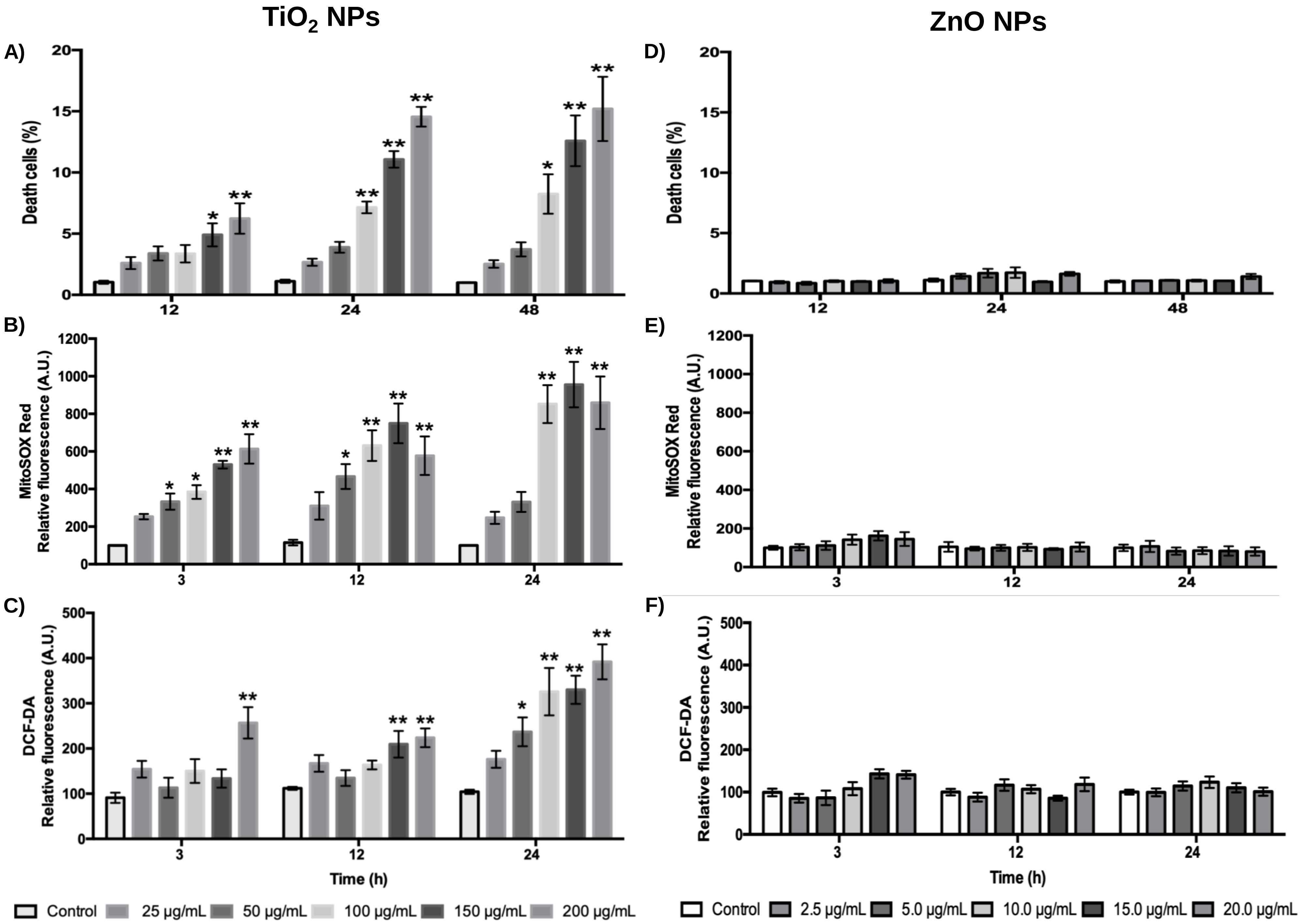

Figure 4. Cytotoxicity determination and ROS generation after TiO_2 NPs or ZnO NPs exposure. Cell viability by PI (A and D) assay and the generation of superoxide anion (B adn E) or H_2O_2 (C and F) were determined after different exposure times to increasing concentracios of TiO_2 NPs or ZnO NPs. Each bar represents the mean values of 3 different experiments ± SEM; *$p < 0.05$, **$p < 0.001$* versus untreated cells. ANOVA, post hoc Bonferroni.

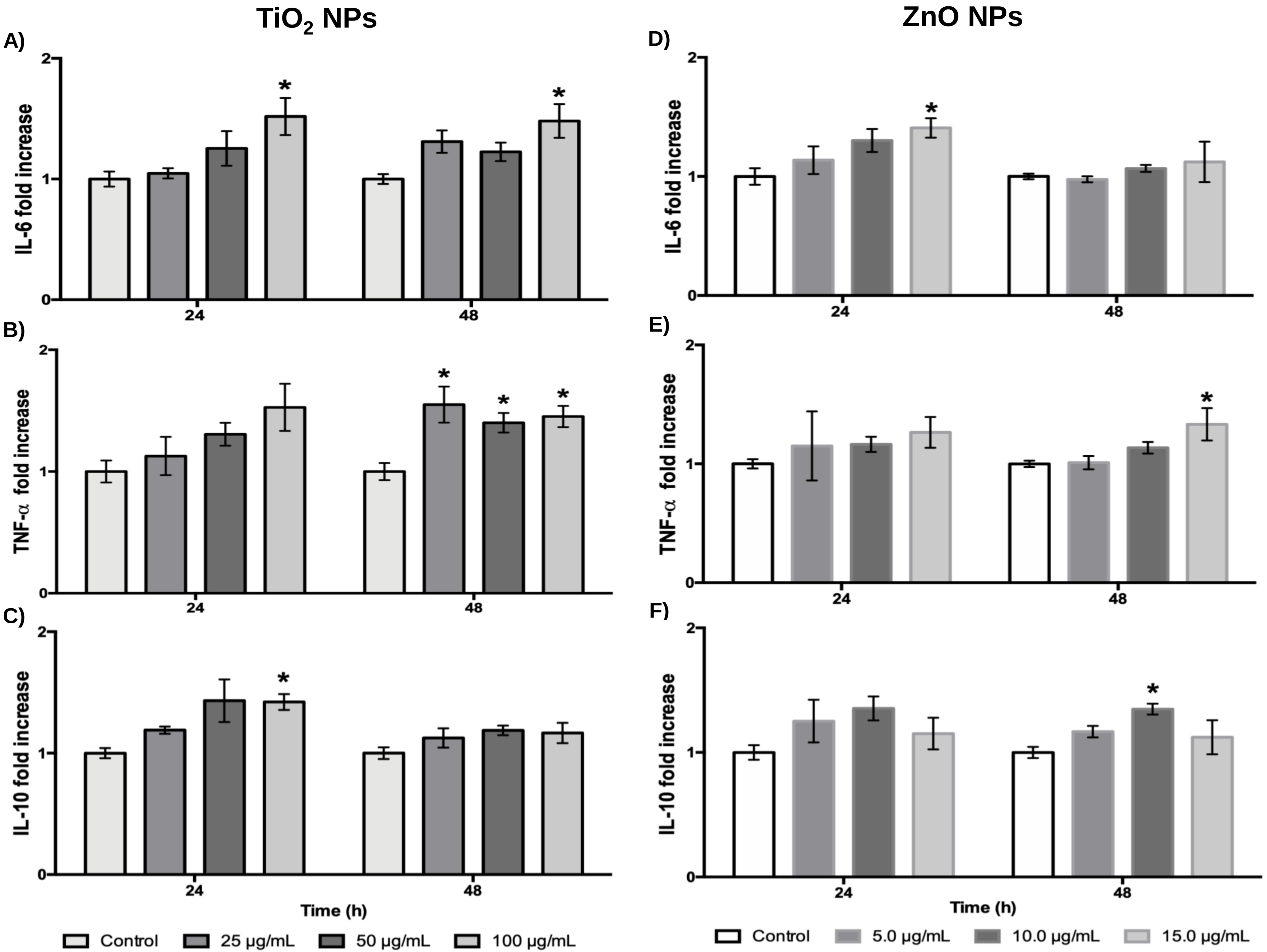

Figure 5. Released cytokines from the A549 cells after TiO_2 NPs or ZnO NPs exposure. The release of the IL-6 (A and D) TNF-α (B and E) or IL-10 (C and F) after different times of exposure to increasing concentración of TiO_2 NPs or ZnO NPs. Each bar represents the mean values of 3 independent experiments ± SEM; $*p < 0.05$, $**p < 0.001$ versus untreated cells. ANOVA, post hoc Bonferroni.

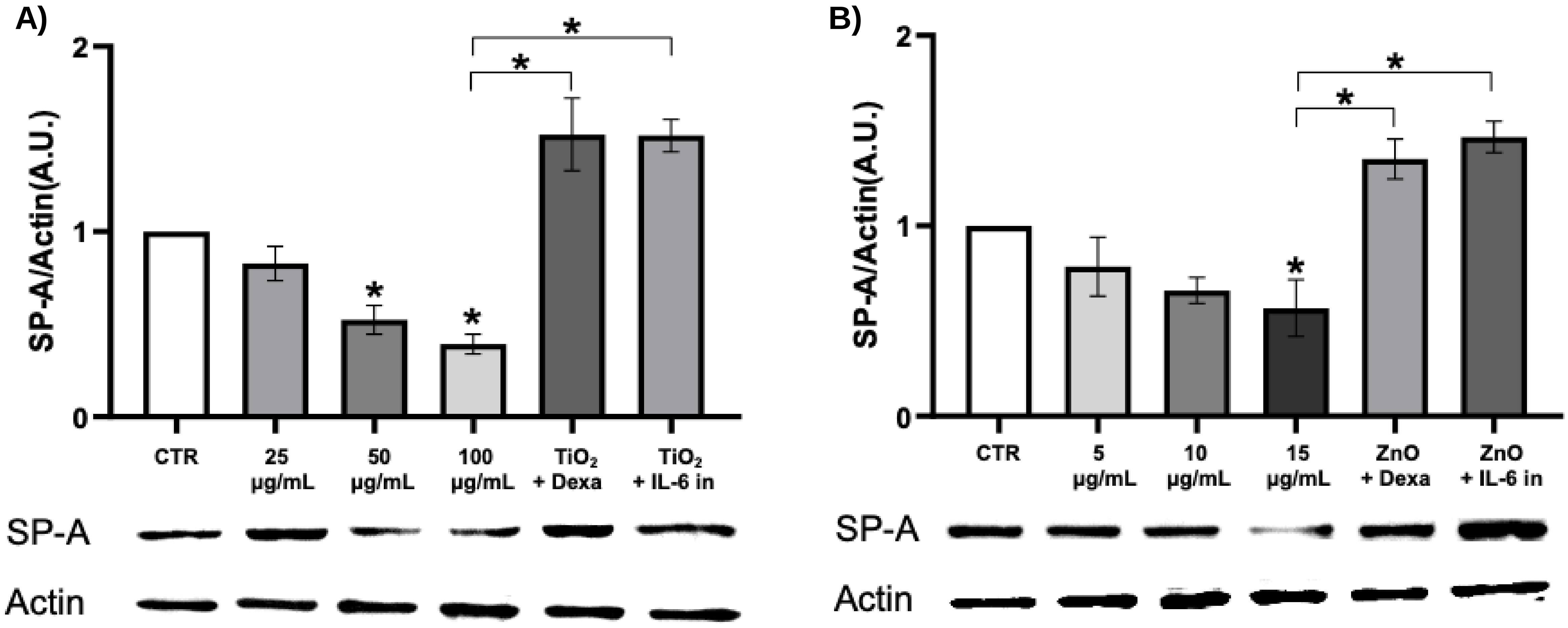

Figure 6. SP-A expression levels after TiO_2 NPs or ZnO NPs exposure. The expression of the surfactant protein A by Western blot was determined after 24 h of exposure to different concentrations of TiO_2 NPs (A) or ZnO NPs (B). To determine the influence of the produced IL-6 after NPs exposure in the SP-A inhibition, the treated cells with 100 µg/mL of TiO_2 NPs or 15 µg/mL of ZnO NPs were co-exposed to the inhibitors anti IL-6 antibody or dexamethasone. Each bar represents the mean value of 3 independent experiments ± SEM; *$p < 0.05$, versus untreated cells or treated cells vs. co-exposure treatments. U-Mann Whitney.

Table revised version

Table 1. Nanoparticles physicochemical characteristics.

NP	TEM size (nm)	Water			Ham´s F12 medium							Endotoxin level (EU/mL)
		Effective density (mg/mL)	DLS(nm) / PDI	Zeta potential (mV)	Effective density (mg/mL)	0 h		24 h		48 h		
						DLS(nm) / PDI	Zeta potential (mV)	DLS(nm) / PDI	Zeta potential (mV)	DLS(nm) / PDI	Zeta potential (mV)	
TiO_2	22 ± 6.51	1.9056	17.06 ± 1.43 / 0.32	0.16 ± 0.30	1.3466	335.97 ± 28.33 / 0.201	-12.07 ± 0.68	369.2 ± 26.4 / 0.19	-12.17 ± 0.98	369.83 ± 28.16 / 0.209	-11.43 ± 0.97	> 0.1
ZnO	16 ± 4.58	1.581	278.33 ± 7.38 / 0.25	30.56 ± 2.22	1.4968	368.57 ± 24.45 / 0.62	-12.2 ± 0.46	207.5 ± 2.26 / 0.77	-11.33 ± 1.67	145.3 78.9 / 0.61	-13.07 ± 1.0	> 0.1

Note: Values represent the mean in triplicate ± standard deviation.

Table 2. Nanoparticles concentration in A549 cells or media.

TiO_2 NPs concentration	Media	Cells	ZnO NPs concentration	Media	Cells
25 µg/mL	3.99	2.23	5 µg/mL	273.23	43.85
50 µg/mL	3.65	4.15	10 µg/mL	975.78	64.22
100 µg/mL	5.06	13.14	15 µg/mL	1841.68	89.74

Concentration values in culture media or cells are in ng/mL. Mean value from a tripicate.

Author contributions

A.J.C. and A.D.V.R. designed the study; A.J.C., A.S.R, and D.L. performed the characterization of the nanoparticles; A.J.C., V.E.R., A.S.R., M.U.R. and R.M.R. performed *in vitro* experiments; A.J.C., L.A.M. and L.C.V. performed and analyzed the metal ions concentrations, A.J.C. and I.E.M.R. performed and analyzed the NPs and cells interaction by atomic force microscopy; A.J.C., A.D.V.R., and F.R.C. performed the data analysis and wrote the manuscript. All the authors revised and approved the manuscript.